



Published in final edited form as:

Trends Cardiovasc Med. 2017 October ; 27(7): 463–472. doi:10.1016/j.tcm.2017.05.003.

Recording Sympathetic Nerve Activity from the Skin

Thomas H. Everett IV, PhD, Anisiia Doytchinova, MD, Yong-Mei Cha, MD*, and Peng-Sheng Chen, MD

Krannert Institute of Cardiology and Division of Cardiology, Department of Medicine, Indiana University School of Medicine, Indianapolis, IN

*Division of Cardiovascular Diseases, Mayo Clinic, Rochester, MN

Abstract

Sympathetic tone is important in cardiac arrhythmogenesis; however, methods to estimate sympathetic tone are either too invasive or require proper sinus node function that may be abnormal in disease states. Because of the direct and extensive connections among various nerve structures, it is possible for the sympathetic nerves in the various structures to activate simultaneously. Therefore, we hypothesized that nerve activity can be recorded from the skin and it can be used to estimate the cardiac sympathetic tone. Preclinical studies in canines demonstrated that nerve activity is detectable using conventional ECG electrodes and can be used to estimate cardiac sympathetic tone. Subsequent clinical studies further supported this concept. In addition to studying the autonomic mechanisms of cardiac arrhythmia, these new methods may have broad application in studying both cardiac and non-cardiac diseases.

Keywords

sympathetic nerve activity; autonomic nervous system; arrhythmia

Introduction

Since the invention of the electrocardiogram (ECG) by Einthoven et al.,⁽¹⁾ the ECG has been an important part of clinical practice. A primary reason for the popularity of the ECG is that it is non-invasive and can be performed in any patient by placing electrodes on the skin. The present methods of ECG recording focus on detecting electrical signals from the heart. However, we hypothesized that the application of the ECG could be expanded to also record sympathetic nerve activity (SNA).

Corresponding Author: Thomas H. Everett, IV, PhD, 1800 N. Capitol Ave, E400E Indianapolis, IN 46202, Phone: 317-274-0957, theveret@iu.edu.

Publisher's Disclaimer: This is a PDF file of an unedited manuscript that has been accepted for publication. As a service to our customers we are providing this early version of the manuscript. The manuscript will undergo copyediting, typesetting, and review of the resulting proof before it is published in its final citable form. Please note that during the production process errors may be discovered which could affect the content, and all legal disclaimers that apply to the journal pertain.

Disclosures: Peng-Sheng Chen has equity interest in Arrhythmotech, LLC. Medtronic, St Jude and Cyberonics Inc. donated research equipment to Dr Chen's research laboratory.

Sympathetic tone is important in cardiac arrhythmogenesis,(2, 3) and a commonly used method to estimate cardiac autonomic nerve activity is to calculate heart rate variability, or sympathetic nerve activity can be directly measured by microneurography.(4, 5) However, these methods are either too invasive and cannot be done in ambulatory subjects or require proper sinus node response to autonomic stimulation which may be abnormal in disease states,(6, 7) and may not reflect the sympathetic tone in those conditions.(8)

Cardiac sympathetic innervation comes from the paravertebral cervical and thoracic ganglia.(9) Among them, the stellate (cervicothoracic) ganglion is a major source of sympathetic innervation. It connects constantly with phrenic nerves and almost as often to the vagal nerves.(9) The paravertebral ganglia also directly connect with spinal nerves,(10) which connect with the intercostal nerves.(11) These intercostal nerves split into ramus cutaneous lateralis and a deep branch to the musculus rectus abdominis.(12) Histological studies of human skin biopsy confirmed the presence of abundant sympathetic nerves in arteriovenous anastomoses, arrector pilorum muscles, and arterioles.(13) Using horseradish peroxidase as tracer, Baron et al(14) and Taniguchi et al(15) found that all skin sensory and sympathetic neurons are located ipsilaterally. The sympathetic somata are located in the middle cervical and stellate ganglia as well as the thoracic ganglia. Because of the direct and extensive connections among various nerve structures, it is possible for the sympathetic nerves in the various structures to activate simultaneously. Therefore, we hypothesized that SNA recorded from the upper thorax can be used to estimate the cardiac sympathetic tone and that this nerve activity could be recorded from the skin.

To preserve the signal from the ECG and eliminate noise, the American Heart Association (AHA) standard recommendation for low pass filtering of the ECG is 150 Hz for adolescents and adults, and 250 Hz for children.(16) Higher frequency signals, although known to be clinically important,(17) are routinely eliminated by this low pass filtering. Because there is no need to record high frequency signals, the conventional ECG and Holter monitoring devices do not have a wide bandwidth and high sampling rate. The high frequency signals that are eliminated may contain both muscle and nerve activities. McAuley et al(18) reported that the electromyography (EMG) usually has a frequency of <100 Hz. At most, small amounts of muscle activity could reach 400 Hz.(19) The standard high pass setting for observing nerve activity during a microneurography study is 700 Hz.(20) Using equipment with a wide bandwidth (2 KHz) and high sampling rates (4K/s–10K/s) we hypothesized that nerve activity could be simultaneously recorded along with the ECG. Signals recorded from electrodes on the skin are band passed between 0.5 Hz and 150 Hz to display ECG signal. The same signals can then be high passed filtered to reveal nerve activity. Data supplement Figure 1 illustrates the above concept. It shows Fast Fourier Transform (FFT) analyses of the signals recorded from the skin. High pass filtering at 150 Hz eliminated the ECG signals. High pass filtering at 500 or 700 Hz increased the specificity but reduced the sensitivity of any nerve recordings. The signal to noise ratio is reduced. However, the basic patterns of nerve discharges remain.

Recently, methods have been developed to record autonomic nerve activity in ambulatory dogs, and through this process, it has been documented that sympathetic nerve activity immediately precedes the onset of atrial and ventricular arrhythmias as well as sudden

cardiac death.(21–24) These methods have included to directly record sympathetic nerve activity from either subcutaneous tissues or on the surface of the skin in canine models. We found that both subcutaneous nerve activity (SCNA) and superficial skin sympathetic nerve activity (SKNA) closely correlate with stellate ganglia nerve activity (SGNA) in ambulatory canine models.(25–27) From these results, we hypothesized that with high frequency sampling and high pass filtering, we can also record SNA from the skin or subcutaneously just underneath the skin in the clinical setting.

Preclinical studies in ambulatory dogs

In an initial series of experiments, a radiotransmitter (D70-EEE, Data Sciences International, St. Paul, MN) was implanted in dogs to record SGNA and vagal nerve activity (VNA).(23, 24, 28, 29) A third pair of bipolar electrodes was placed in the subcutaneous space, with one electrode each inserted under the subcutaneous tissue of left thorax and left abdomen. After 2 weeks of recovery, the radiotransmitter was turned on to continuously record from all 3 electrodes at a sampling rate of 1,000 Hz. To optimize nerve signals and to filter out any residual ECG signals, data from the left stellate ganglion, the left thoracic vagus nerve, and the subcutaneous tissue were high-pass filtered at 150 Hz and simultaneously displayed with the low pass (100 Hz) filtered ECG from subcutaneous recording.

Episodes of supraventricular (sinus or atrial) tachycardia were defined as heart rate exceeding 150 bpm with narrow QRS complexes. The first 10 tachycardia episodes in which the recordings showed no evidence of noise or motion artifacts were selected for analysis.

Subcutaneous SNA in ambulatory dogs

Auditory excitation was used to trigger canine sympathetic nerve discharges. There were electrical signals resembling nerve activities in the subcutaneous tissues of all dogs studied. Manual analyses showed that a vast majority of these electrical signals represented subcutaneous nerve activity (SCNA). The beginning of the recording shown in Figure 1A shows heart rate variations consistent with baseline respiratory heart rate (RHR) responses commonly observed in dogs.(30) The respiratory heart rate responses were followed by a sustained increase of heart rate exceeding 150 bpm (upward arrow) and simultaneous SGNA and SCNA (downward arrows). There were no RHR during these nerve activities. The RHR resumed after the bursts of nerve activities terminated. Figure 1B shows similar activities that occurred 25 s later in the same dog. Again, the SGNA was associated with sustained heart rate elevation that exceeded 150 bpm. All episodes had regular narrow QRS complexes preceded by distinct P waves, consistent with supraventricular tachycardia (including sinus tachycardia). It was found that both SGNA and SCNA invariably preceded these supraventricular tachycardia episodes.

Integrated nerve activities and heart rate

To quantify the high frequency discharges that are associated with nerve activity, the integrated nerve activity is calculated by integrating the amplitude of nerve activity over time (minute by minute). In the study described above, integrated SCNA (iSCNA) correlated positively with integrated SGNA (iSGNA) in all dogs analyzed. In addition, the correlation between heart rate and iSCNA (average $r=0.74$, 95% CI 0.68 to 0.80, $N=7$) was significantly

better than the correlation between heart rate and iSGNA (average $r=0.56$, 95% CI 0.45 to 0.67, $N=7$, $p=0.0135$) in all dogs studied.

Dogs with myocardial infarction and complete heart block

In a study performed in dogs with myocardial infarction, complete heart block and nerve growth factor infusion to the left stellate ganglion, most of the ventricular tachycardia (86.3%) and sudden cardiac death were preceded within 15 seconds by SGNA.(24) One of the recording channels was in the left thoracic subcutaneous space for ECG recordings. Signals were recorded from 6 dogs and filtered with a 150 Hz high-pass filter. The results showed that all dogs had VT and 2 dogs died suddenly of VF. Both VF episodes were preceded by nearly continuous SCNA (150 s and 150 s) and SGNA (42 s and 42 s). There was SCNA within 15 s before 33 (76.7%) of 43 VT episodes. An example of increased nerve activity preceding ventricular fibrillation is shown in Data Supplement Figure 2.

Significantly progressive increase in integrated SGNA (in mV-s, 76.4 ± 54.7 , 82.0 ± 50.5 , 95.4 ± 57.7) and SCNA (89.1 ± 50.8 , 98.5 ± 52.9 and 111.1 ± 59.3) was observed 60 s, 40 s and 20 s, respectively, prior to VT/VF ($p<0.001$ for both).

Comparing SGNA to SCNA and SKNA

Even though SCNA correlated well with SGNA as demonstrated in the studies described above, a skin incision is still needed for implanting the subcutaneous electrodes. For clinical applications, it is highly desirable to develop a completely non-invasive method for direct skin sympathetic nerve recording. We hypothesized that it is possible to record SKNA from the surface of the skin in dogs, and that the SKNA recorded from the upper chest wall can be used to estimate the SGNA. In order to test this hypothesis, studies were performed in canines that directly measured SGNA, along with SCNA, and SKNA with electrodes on the skin. A pair of bipolar electrodes were inserted under the fascia of the right stellate ganglion to record SGNA as the “gold standard” of sympathetic tone. Electrocardiogram (ECG) patches (Tyco/Healthcare Kendall, Medi-Trace 100, Hampshire, U.K.) were secured on the skin using adhesive tapes to record ECG Leads I and II as shown in Figure 3 of the Data Supplement. An additional patch was secured to the right lower abdomen to serve as ground. To explore whether or not other locations on the chest wall can also be used for SKNA recording, we placed one pair of bipolar electrodes each at the level of the right and left 3rd rib in to form bipolar electrode recordings with 12 cm interelectrode distance. Signals from these electrodes were recorded at a bandwidth set at 10 Hz-3 KHz, and digitized at 10,000 Hz. After all surgical procedures were completed, the anesthetic agents were switched from isoflurane to alpha-chloralose (up to 100 mg/kg) and morphine. Apamin (1 ml, concentration 0.2 ng/ μ L) was then injected directly into the right stellate ganglion. Apamin, a neurotoxin, is a specific blocker of the small conductance calcium activated K (SK) channel.(31) Inhibition of the SK channel is known to facilitate neuronal discharges.(32, 33) Data was acquired for 10 min after apamin injection. Signals recorded from the skin electrodes were high-pass filtered at 150 Hz to display SKNA and low pass filtered at 30 Hz to display the surface ECG. The latter was then used for heart rate analyses. Quantitative analyses was performed by integrating SGNA (iSGNA), and SKNA (iSKNA) min by min. Apamin injection induced robust activity of SKNA and SGNA in all dogs studied. Data Supplement Figure 4 shows nerve activity after apamin injection. The figure also shows

significantly positive correlations among integrated left SGNA (iLSGNA) and iSKNA-I, iSKNA-II, iSKNA-R, iSKNA-L and heart rate in this dog. For all dogs studied, there were consistently strong and significant ($p < 0.05$) positive correlations (mean r value of 0.877, range from 0.745 to 0.985) found between iSGNA and iSKNA-I. Both right and left integrated SGNA (iRSGNA and iLSGNA) correlated well with the ipsilateral integrated SKNA (iRSKNA and iLSKNA) respectively. These findings suggest that SCNA and SKNA may be used as a surrogate of SGNA in detecting elevated sympathetic tone. This data supported the feasibility of recording sympathetic nerve discharges from skin.

Clinical Studies

The studies outlined above indicated that SKNA can be used to estimate SGNA in ambulatory dogs. Based on those results, we hypothesized that it is feasible to simultaneously record SKNA and the ECG in humans. To test this hypothesis, we recorded signals from four different groups of patients and the results are outlined below. The research protocols were approved by the Institutional Review Board (IRB) of the Indiana University School of Medicine. All subjects gave informed consent to participate. Data were prospectively collected and analyzed. All recordings were made using standard ECG electrodes placed as shown in Figure 2 and connected to recording devices that included a ML138 or ML135 OctoBioAmp (ADInstruments, Colorado Springs, CO) or a portable ME6000 (Biomation, Ontario, Canada) device with a wide bandwidth (> 1 K Hz) and high sampling rate (4–10 K/s). The average impedance of the electrodes measured 37 ± 8 k Ω (range 28–52 k Ω). The results of how different filter setting affect the signal to noise ratio is shown in Figure 3.

Healthy Volunteers Undergoing Provocative Maneuvers

We enrolled 12 healthy volunteers (5 female, age 32 ± 7) for SKNA recording during the cold water pressor test (CWPT) and Valsalva maneuver (VM), which are maneuvers known to increase sympathetic tone.⁽²⁰⁾ Among them, 9 completed the CWPT, including 8 who also completed the VM. The CWPT was performed by placing subject's left hand up to the wrist in iced water for 2 minutes.⁽²⁰⁾ The subjects also performed the VM by blowing into the mouthpiece of a sphygmomanometer aiming to sustain 35 mmHg of pressure for 30 s.⁽³⁴⁾ A two minute control and recovery period were recorded for both maneuvers.

Both CWPT and VM resulted in increased blood pressure and HR. Figure 4 shows the tracing of a subject at baseline (panels A and B) and during the Valsava maneuver (panels C and D). Figure 4A shows that spontaneous bursts of nerve activity were associated with an elevated HR, and figure 1B shows basal state nerve discharges. Figures 4C and D show the effects of performing the Valsava maneuver on the SKNA. As the figures show, the Valsava maneuver increased SKNA. When the signals are magnified (Figure 4D), neither the SKNA (first line) nor integrated SKNA (third line) appears to synchronize with the heart rate (second line). Figure 5 shows the resulting recordings during the CWPT from subjects 1–4 recorded in a bipolar lead I configuration, which showed that SKNA increased immediately after immersion and remained elevated throughout the test with quick offset after the stimulus is removed. Few bursts were noted prior to immersion consistent with sympathetic activation in anticipation of a painful stimulus.

Continuous neuECG Monitoring in Patients Without Heart Diseases

We continuously recorded SKNA in 19 patients (12 female, ages 36 ± 11 years) without known heart diseases admitted to the video electroencephalography unit for seizure recurrence monitoring while off antiepileptic therapy. We selected a consecutive 24-hour seizure free period for analyses to determine the relationship between SKNA and spontaneous HR acceleration. We analyzed the first 10 episodes of SKNA per patient. In addition, we determined QT and QTc intervals using the Bazett's formula.(35) A total of 190 (10 per patient) sympathetic nerve discharges detected in bipolar ECG lead I placed on the chest were selected for analyses. SKNA increased the HR from 72 ± 7 bpm to 93 ± 11 bpm ($p<0.001$) (Figure 6). The SKNA shortened the QT interval from 387 ± 24 ms to 369 ± 24 ms ($p<0.001$). These findings are consistent with the normal responses of QT intervals during sympathetic activation.(36)

Sympathetic Nerve Activity and Ventricular Tachycardia

We recorded SKNA from 22 patients (7 female, age 60.6 ± 14) admitted to the hospital with electrical storm (ES).(37) The recording lasted for 39.0 ± 28.2 hours, and approximately 50% of the patients were sedated during the recordings. The percentage of spontaneously occurring VT or VF episodes that were preceded within 30 s by SKNA reaching signal to noise ratio of 2:1 was reported. Thirty second control periods were selected 20 min after the onset of the VT episode. The frequency of nerve discharges during the control period was reported. Ten of the 22 patients had recurrent VT on the recording, one of which was predominantly in incessant hemodynamically stable VT. The other 9 patients accounted for a total of 146 separate VT episodes with a HR of 208 ± 68 bpm and duration of 34 ± 253 s (range 1–2983 s). The majority of those episodes were non-sustained with sustained (> 30 seconds or requiring therapy) VT representing only 8%. Many SKNA discharges were observed during sustained VT (Figure 7A). Out of the 146 VT episodes in the remaining 9 patients, 73% were preceded by discharges in lead I (Figure 7B). By using generalized linear mixed model, the odds ratio of having discharge 30 s before the VT versus during the 30 s control periods for a specific patient as detected by lead I was 7.45 [95% CI 3.14–17.72], $p<0.0001$). No significant difference was noted for lead II.

Ganglionic Blockade

We studied a 61 year old man and a 53 year old man with ischemic cardiomyopathy and a 71 year old man with arrhythmogenic right ventricular cardiomyopathy. They underwent bilateral stellate ganglion injection with 2% lidocaine (10 ml) while SKNA was being recorded. The injection protocol included inserting needles under fluoroscopic guidance and local contrast injection to ascertain the location of the needle. During these procedures, the patient had significant SKNA activation. Lidocaine injection into the stellate ganglia reduced SKNA in all 3 patients studied (Figure 8).

Limitations

We are obtaining our recordings from normal ECG electrodes that are placed on the skin. These large surface area electrodes can be influenced by signals from a wide variety of nerve structures, and can contain activity from both the parasympathetic and sympathetic nervous

systems. We have compared our skin nerve activity recordings (SKNA) to direct recordings from the stellate ganglion and demonstrated a strong correlation. However, we have not analyzed the contribution of nerve activity outside of the sympathetic nervous system to these recordings. In addition, even though the presence of nerve activity has been correlated to changes in heart rate, the correlation between amplitude and duration of the nerve recordings to changes in heart rate has not been evaluated. In addition, correlations between nerve activity and cardiac sympathetic neurotransmitters, blood pressure, cardiac output, and other hemodynamic parameters remains to be investigated. The absolute SKNA reported in our study differs than the absolute SSNA reported in microneurography studies. We calculated the absolute SKNA by averaging the voltage of digitized signals and reported the results as μV per sample. However, in the microneurography literature, the number of bursts per unit time was used to quantitate the sympathetic nerve activity. Young et al(38) suggested that it is more difficult to use the frequency of bursts to quantitative skin sympathetic nerve activity (SSNA) than muscle sympathetic nerve activity (MSNA) measured with microneurography. It is possible that the same limitation also applies to SKNA recording. More data are needed to determine if the μV values of SKNA can be used to compare the sympathetic tone among different individuals.

Conclusion

From the studies outlined above, we conclude that SKNA is detectable using conventional ECG electrodes and can be used to estimate cardiac sympathetic tone. Because the left stellate ganglion nerve activity (SGNA) is known to trigger cardiac arrhythmias, including AF, VT and VF,(23, 24, 39) it is possible that skin SNA can also be used for arrhythmia prediction. In addition to studying the autonomic mechanisms of cardiac arrhythmia, these new methods may have broad application in studying both cardiac and non-cardiac diseases. For example, sympathetic tone is important in the pathogenesis of heart failure,(40) atherosclerosis,(41) peripheral neuropathies,(42) epilepsy,(43) vasovagal syncope,(44) renal failure,(45) hypertension(46) and many others diseases. Direct SKNA and SCNA recording may provide new approaches to study the mechanisms of these common diseases. SKNA recording may also have immediate clinical applications by assisting in the diagnosis and treatment of hyperhidrosis (sweaty palms), paralysis, stroke, diabetes, and neuromuscular diseases. It may be used to assist biofeedback monitoring performed by neurologists to control neuropsychiatric disorders.

Supplementary Material

Refer to Web version on PubMed Central for supplementary material.

Acknowledgments

Sources of Funding

Supported by NIH grants R41 HL124741, R42 DA043391 (Dr Everett), P01 HL78931, R01 HL71140 (Dr Chen), Indiana University School of Medicine Biomedical Research Grant, a Charles Fisch Cardiovascular Research Award endowed by Dr Suzanne B. Knoebel of the Krannert Institute of Cardiology (Dr Everett), a Medtronic-Zipes Endowment and the Indiana University Health-Indiana University School of Medicine Strategic Research Initiative (Dr Chen).

References

1. Einthoven, W. Galvanometrische registratie van het menselijk electrocardiogram. Leiden, Netherlands: Eduard Ijdo; 1902.
2. Rubart M, Zipes DP. Mechanisms of sudden cardiac death. *JClinInvest*. 2005; 115(9):2305–15.
3. Shen MJ, Choi EK, Tan AY, Lin SF, Fishbein MC, Chen LS, et al. Neural mechanisms of atrial arrhythmias. *Nat Rev Cardiol*. 2011; 27:30–9.
4. Mark AL, Wallin BG. Microneurography: a technique for assessing central neural effects of adrenergic drugs on sympathetic outflow in humans. *J Cardiovasc Pharmacol*. 1985; 7(Suppl 8):S67–9.
5. Vallbo AB, Hagbarth KE, Wallin BG. Microneurography: how the technique developed and its role in the investigation of the sympathetic nervous system. *JApplPhysiol*. 2004; 96(4):1262–9.
6. Sanders P, Kistler PM, Morton JB, Spence SJ, Kalman JM. Remodeling of sinus node function in patients with congestive heart failure: reduction in sinus node reserve. *Circulation*. 2004; 110(8):897–903. [PubMed: 15302799]
7. Hocini M, Sanders P, Deisenhofer I, Jais P, Hsu LF, Scavee C, et al. Reverse remodeling of sinus node function after catheter ablation of atrial fibrillation in patients with prolonged sinus pauses. *Circulation*. 2003; 108(10):1172–5. [PubMed: 12952840]
8. Piccirillo G, Ogawa M, Song J, Chong VJ, Joung B, Han S, et al. Power spectral analysis of heart rate variability and autonomic nervous system activity measured directly in healthy dogs and dogs with tachycardia-induced heart failure. *Heart Rhythm*. 2009; 6(4):546–52. [PubMed: 19324318]
9. Ellison JP, Williams TH. Sympathetic nerve pathways to the human heart, and their variations. *Am J Anat*. 1969; 124(2):149–62. [PubMed: 5774648]
10. Kawashima T. The autonomic nervous system of the human heart with special reference to its origin, course, and peripheral distribution. *AnatEmbryol(Berl)*. 2005; 209(6):425–38.
11. Ramsaroop L, Partab P, Singh B, Satyapal KS. Thoracic origin of a sympathetic supply to the upper limb: the ‘nerve of Kuntz’ revisited. *J Anat*. 2001; 199(Pt 6):675–82. [PubMed: 11787821]
12. Schalow G, Aho A, Lang G. Microanatomy and number of nerve fibres of the lower intercostal nerves with respect to a nerve anastomosis. Donor nerve analysis. I. (IV). Electromyography and clinical neurophysiology. 1992; 32(4–5):171–85. [PubMed: 1600882]
13. Donadio V, Nolano M, Provitera V, Stancanelli A, Lullo F, Liguori R, et al. Skin sympathetic adrenergic innervation: an immunofluorescence confocal study. *Ann Neurol*. 2006; 59(2):376–81. [PubMed: 16437571]
14. Baron R, Janig W, With H. Sympathetic and afferent neurones projecting into forelimb and trunk nerves and the anatomical organization of the thoracic sympathetic outflow of the rat. *J Auton Nerv Syst*. 1995; 53(2–3):205–14. [PubMed: 7560757]
15. Taniguchi T, Morimoto M, Taniguchi Y, Takasaki M, Totoki T. Cutaneous distribution of sympathetic postganglionic fibers from stellate ganglion: A retrograde axonal tracing study using wheat germ agglutinin conjugated with horseradish peroxidase. *J Anesth*. 1994; 8:441–9. [PubMed: 28921353]
16. Kligfield P, Gettes LS, Bailey JJ, Childers R, Deal BJ, Hancock EW, et al. Recommendations for the standardization and interpretation of the electrocardiogram. Part I: The electrocardiogram and its technology. A scientific statement from the American Heart Association Electrocardiography and Arrhythmias Committee, Council on Clinical Cardiology; the American College of Cardiology Foundation; and the Heart Rhythm Society. *Heart Rhythm*. 2007; 4(3):394–412. [PubMed: 17341413]
17. Langner PH Jr, Geselowitz DB, Briller SA. Wide band recording of the electrocardiogram and coronary heart disease. *Am Heart J*. 1973; 86(3):308–17. [PubMed: 4727268]
18. McAuley JH, Rothwell JC, Marsden CD. Frequency peaks of tremor, muscle vibration and electromyographic activity at 10 Hz, 20 Hz and 40 Hz during human finger muscle contraction may reflect rhythmicities of central neural firing. *Exp Brain Res*. 1997; 114(3):525–41. [PubMed: 9187289]

19. Komi PV, Tesch P. EMG frequency spectrum, muscle structure, and fatigue during dynamic contractions in man. *European journal of applied physiology and occupational physiology*. 1979; 42(1):41–50. [PubMed: 499196]
20. Victor RG, Leimbach WN Jr, Seals DR, Wallin BG, Mark AL. Effects of the cold pressor test on muscle sympathetic nerve activity in humans. *Hypertension*. 1987; 9(5):429–36. [PubMed: 3570420]
21. Jung BC, Dave AS, Tan AY, Gholmieh G, Zhou S, Wang DC, et al. Circadian variations of stellate ganglion nerve activity in ambulatory dogs. *Heart Rhythm*. 2006; 3:78–85. [PubMed: 16399059]
22. Ogawa M, Zhou S, Tan AY, Song J, Gholmieh G, Fishbein MCLH, et al. Left stellate ganglion and vagal nerve activity and cardiac arrhythmias in ambulatory dogs with pacing-induced congestive heart failure. *J Am Coll Cardiol*. 2007; 50:335–43. [PubMed: 17659201]
23. Tan AY, Zhou S, Ogawa M, Song J, Chu M, Li H, et al. Neural mechanisms of paroxysmal atrial fibrillation and paroxysmal atrial tachycardia in ambulatory canines. *Circulation*. 2008; 118:916–25. [PubMed: 18697820]
24. Zhou S, Jung BC, Tan AY, Trang VQ, Gholmieh G, Han SW, et al. Spontaneous stellate ganglion nerve activity and ventricular arrhythmia in a canine model of sudden death. *Heart Rhythm*. 2008; 5(1):131–9. [PubMed: 18055272]
25. Robinson EA, Rhee KS, Doytchinova A, Kumar M, Shelton R, Jiang Z, et al. Estimating Sympathetic Tone by Recording Subcutaneous Nerve Activity in Ambulatory Dogs. *J Cardiovasc Electrophysiol*. 2014; 26:70–8. [PubMed: 25091691]
26. Doytchinova A, Patel J, Zhou S, Chen H, Lin S-F, Shen C, et al. Subcutaneous nerve activity and spontaneous ventricular arrhythmias in ambulatory dogs. *Heart Rhythm*. 2015; 12(3):612–20.
27. Jiang Z, Zhao Y, Doytchinova A, Kamp NJ, Tsai WC, Yuan Y, et al. Using skin sympathetic nerve activity to estimate stellate ganglion nerve activity in dogs. *Heart Rhythm*. 2015; 12(6):1324–32. [PubMed: 25681792]
28. Choi E-K, Shen MJ, Han S, Kim D, Hwang S, Sayfo S, et al. Intrinsic cardiac nerve activity and paroxysmal atrial tachyarrhythmia in ambulatory dogs. *Circulation*. 2010; 121:2615–23. [PubMed: 20529998]
29. Ogawa M, Zhou S, Tan AY, Song J, Gholmieh G, Fishbein MCLH, et al. Left stellate ganglion and vagal nerve activity and cardiac arrhythmias in ambulatory dogs with pacing-induced congestive heart failure. *Journal of the American College of Cardiology*. 2007; 50:335–43. [PubMed: 17659201]
30. McCrady JD, Vallbona C, Hoff HE. Neural origin of the respiratory-heart rate response. *Am J Physiol*. 1966; 211(2):323–8. [PubMed: 5921094]
31. Adelman JP, Maylie J, Sah P. Small-Conductance $\text{Ca}(2+)$ -Activated $\text{K}(+)$ Channels: Form and Function. *Annu Rev Physiol*. 2012; 74:245–69. [PubMed: 21942705]
32. Grillner S. The motor infrastructure: from ion channels to neuronal networks. *Nat Rev Neurosci*. 2003; 4(7):573–86. [PubMed: 12838332]
33. Robinson EA, Rhee KS, Doytchinova A, Kumar M, Shelton R, Jiang Z, et al. Estimating sympathetic tone by recording subcutaneous nerve activity in ambulatory dogs. *J Cardiovasc Electrophysiol*. 2015; 26(1):70–8. [PubMed: 25091691]
34. Salmanpour A, Frances MF, Goswami R, Shoemaker JK. Sympathetic neural recruitment patterns during the Valsalva maneuver. *Conf Proc IEEE Eng Med Biol Soc*. 2011; 2011:6951–4. [PubMed: 22255937]
35. Luo S, Michler K, Johnston P, Macfarlane PW. A comparison of commonly used QT correction formulae: the effect of heart rate on the QTc of normal ECGs. *J Electrocardiol*. 2004; 37(Suppl): 81–90. [PubMed: 15534815]
36. Viskin S, Postema PG, Bhuiyan ZA, Rosso R, Kalman JM, Vohra JK, et al. The response of the QT interval to the brief tachycardia provoked by standing: a bedside test for diagnosing long QT syndrome. *J Am Coll Cardiol*. 2010; 55(18):1955–61. [PubMed: 20116193]
37. Gatzoulis KA, Andrikopoulos GK, Apostolopoulos T, Sotiropoulos E, Zervopoulos G, Antoniou J, et al. Electrical storm is an independent predictor of adverse long-term outcome in the era of implantable defibrillator therapy. *Europace*. 2005; 7(2):184–92. [PubMed: 15763536]

38. Young CN, Keller DM, Crandall CG, Fadel PJ. Comparing resting skin sympathetic nerve activity between groups: caution needed. *J Appl Physiol* (1985). 2009; 106(5):1751–2. author reply 3. [PubMed: 19414629]
39. Choi EK, Shen MJ, Han S, Kim D, Hwang S, Sayfo S, et al. Intrinsic cardiac nerve activity and paroxysmal atrial tachyarrhythmia in ambulatory dogs. *Circulation*. 2010; 121(24):2615–23. [PubMed: 20529998]
40. Leimbach WN Jr, Wallin BG, Victor RG, Aylward PE, Sundlof G, Mark AL. Direct evidence from intraneural recordings for increased central sympathetic outflow in patients with heart failure. *Circulation*. 1986; 73(5):913–9. [PubMed: 3698236]
41. Swirski FK, Nahrendorf M. Leukocyte behavior in atherosclerosis, myocardial infarction, and heart failure. *Science*. 2013; 339(6116):161–6. [PubMed: 23307733]
42. Donadio V, Liguori R. Microneurographic recording from unmyelinated nerve fibers in neurological disorders: an update. *Clinical neurophysiology: official journal of the International Federation of Clinical Neurophysiology*. 2015; 126(3):437–45. [PubMed: 25457652]
43. Lotufo PA, Valiengo L, Bensenor IM, Brunoni AR. A systematic review and metaanalysis of heart rate variability in epilepsy and antiepileptic drugs. *Epilepsia*. 2012; 53(2):272–82. [PubMed: 22221253]
44. Jardine DL, Ikram H, Frampton CM, Frethey R, Bennett SI, Crozier IG. Autonomic control of vasovagal syncope. *Am J Physiol*. 1998; 274(6 Pt 2):H2110–5. [PubMed: 9841538]
45. Converse RL Jr, Jacobsen TN, Toto RD, Jost CM, Cosentino F, Fouad-Tarazi F, et al. Sympathetic overactivity in patients with chronic renal failure. *N Engl J Med*. 1992; 327(27):1912–8. [PubMed: 1454086]
46. Hansen J, Victor RG. Direct measurement of sympathetic activity: new insights into disordered blood pressure regulation in chronic renal failure. *Curr Opin Nephrol Hypertens*. 1994; 3(6):636–43. [PubMed: 7881990]
47. Doytchinova A, H J, Y Y, Lin H, Yin D, Adams D, et al. Simultaneous non-Invasive Recording of skin sympathetic nerve activity and electrocardiogram. *Heart Rhythm*. 2017; 14:25–33. [PubMed: 27670627]

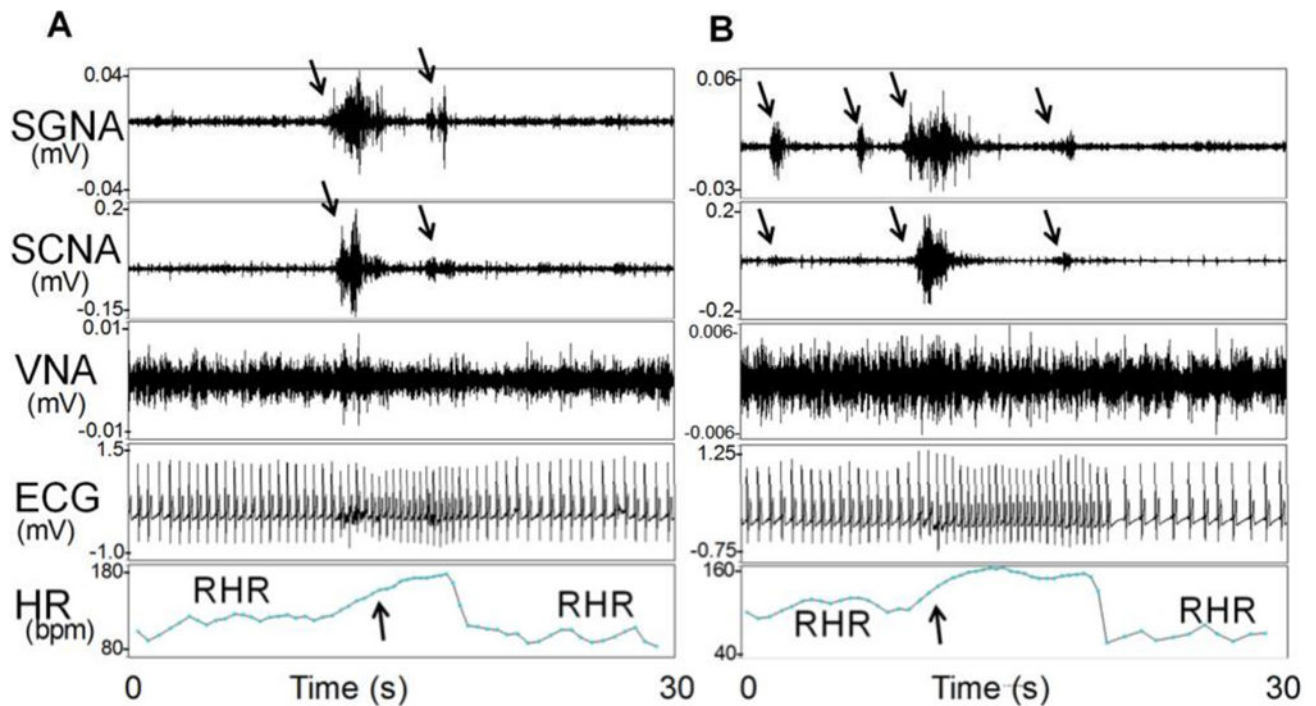


Figure 1. SCNA and SGNA are associated with heart rate elevation in an ambulatory dog. The first portion of Panel A shows rhythmic heart rate (HR) variations consistent with respiratory heart rate responses (RHR). SGNA and SCNA (downward arrows) then activated simultaneously, resulting in heart rate acceleration (upward arrow). There were no obvious changes of VNA in this recording. Simultaneous cessation of the SGNA and SCNA was associated with a reduction of the heart rate and the resumption of RHR. B shows simultaneous activation of SGNA, SCNA (downward arrows) in the same dog 25 seconds after Panel A. Downward arrows point to simultaneous nerve activities in SGNA and SCNA. Upward arrow indicates the onset of tachycardia. ECG, electrocardiogram. (From Robinson et al, J Cardiovasc Electrophysiol; 2015)(33)

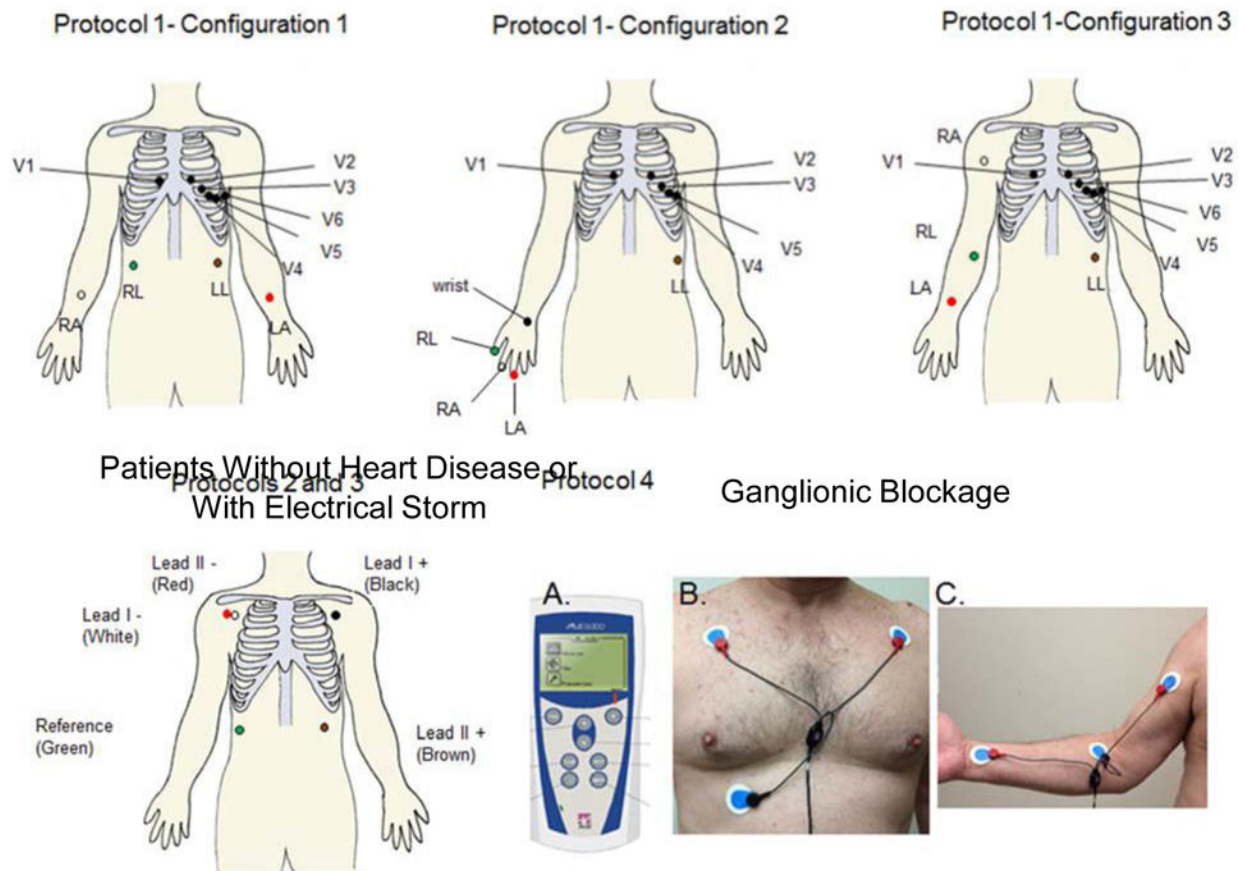


Figure 2.

Electrode locations. We used OctoBioAmp (ADInstruments, Colorado Springs, CO) to record SKNA in healthy volunteers and in patients without heart disease or with electrical storm. We used the healthy volunteer protocol to test various electrocardiogram (ECG) lead positions. All subjects had unipolar recordings from the usual chest lead locations V1–V6, except for three whose lead V1 was moved to the right wrist and leads V2–V6 were shifted in the V1–V5 position for unipolar recording. All bipolar recordings were made with limb lead ECG patch electrodes placed on the arms, abdomen, or fingers. For patients undergoing a bilateral stellate ganglion injection procedure, a portable ME6000 device was used for data acquisition. (A) shows the portable (181 × 85 × 35 mm) ME6000 Biomonitor. One channel was used to record ECG Lead I (B). The red electrodes were placed in the subclavicular area and the black electrode served as reference. A second channel was used to record SKNA from the right arm (C) to avoid ECG contamination. RA=right arm electrode, LA=left arm electrode, RL=right leg electrode (reference), LL=left leg electrode, wrist=unipolar electrode (V1) placed at the wrist location, V1–V6=standard unipolar electrocardiogram leads. (From Online Data Supplement, Doytchinova et al, Heart Rhythm 2017)(47)

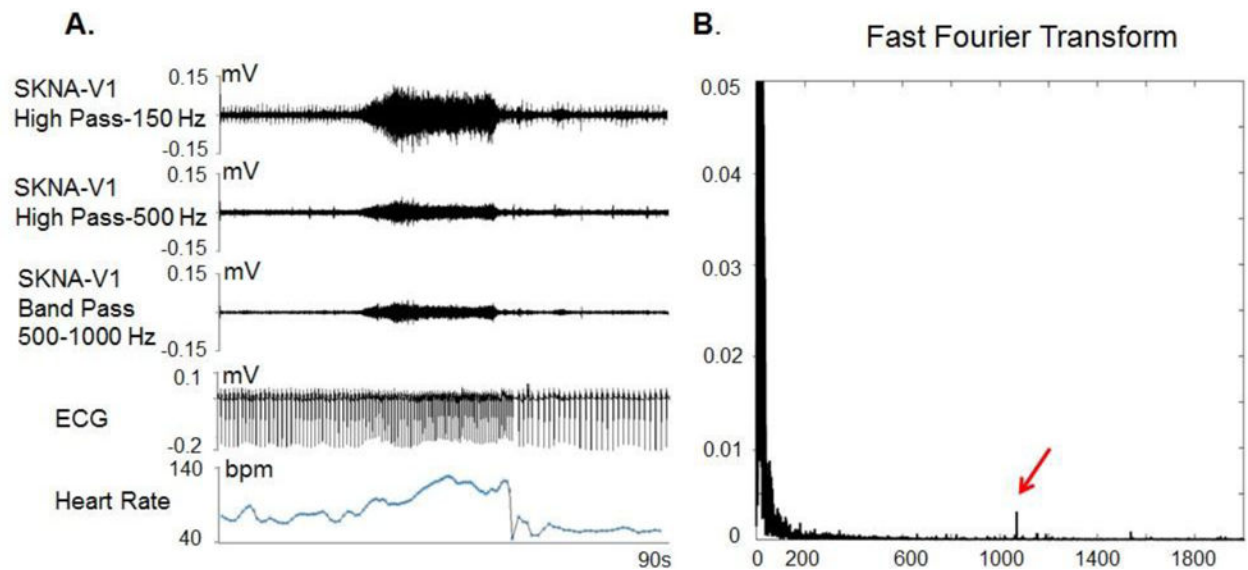


Figure 3.

Filter setting and signal to noise ratio of a recording from a healthy volunteer. Panel A shows the same data filtered with 3 different methods. After applying 150 Hz high pass filter, the ECG signals were incompletely eliminated but the nerve signals are clearly visible with a good signal to noise ratio. After applying the same data with a 500 Hz high pass filter, all ECG signals are eliminated by the signal to noise ratio for the nerve signal is reduced by approximately 50%. A Fast Fourier Transform analyses (Panel B) shows a high power signal (red arrow) slightly higher than 1000 Hz. This high power signal might be noise. Applying a band pass filter between 500 Hz and 1000 Hz eliminated that noise and reduced the thickness of the baseline, hence improved the signal to noise ratio of the SKNA. (From Online Data Supplement, Doytchinova et al, Heart Rhythm 2017)(47)

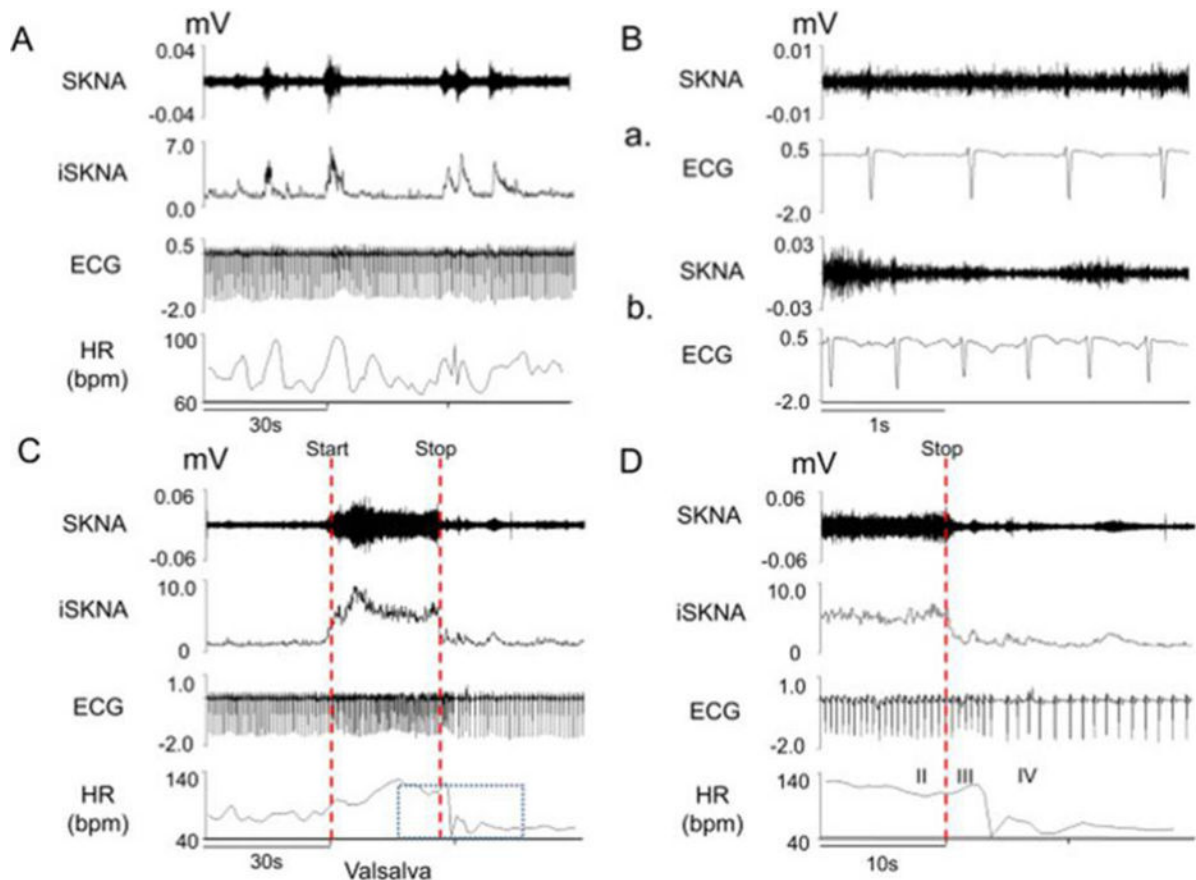


Figure 4. SKNA recordings from a health volunteer undergoing the Valsalva maneuver. Signals from lead V1 were bandpass filtered between 500–1000 Hz to detect SKNA and bandpass filtered between 0.5–150 Hz to detect the ECG. Integrated SKNA (iSKNA) was calculated over a 100-ms window. A: Increased SKNA was associated with heart rate (HR) acceleration. B: Higher magnification of SKNA showing baseline spontaneous nerve activity (a) and large variations of nerve discharges associated with tachycardia (b). C: increased SKNA and HR were evident during Valsalva maneuver. Dotted red lines mark the start and stop of the maneuver. D: Magnified boxed segment from Panel C showing phases II–IV of the Valsalva maneuver, demonstrating that SKNA was not synchronous with the QRS complex. (From Doytchinova et al, Heart Rhythm 2017)(47)

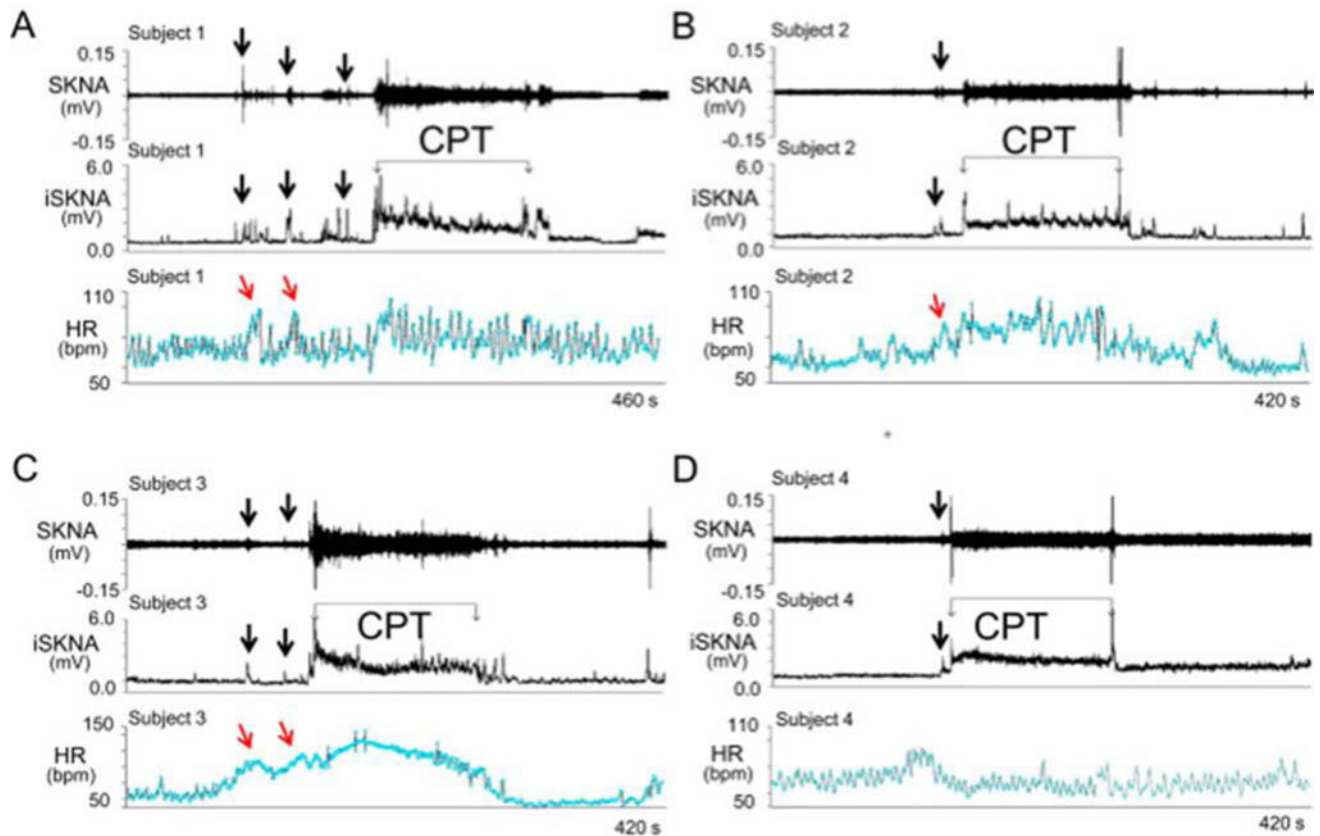


Figure 5.

SKNA recordings during the cold water pressor test (CPT) in healthy volunteers. The electrode location was on the right and left arm for ECG Lead I recording. A–D: Increased skin sympathetic nerve activity (SKNA) was detected in subjects 1–4, respectively, during the CPT. Black downward arrows point to increased SKNA prior to CPT, likely due to the anticipation of the impending cold water immersion. The increased SKNA was associated with heart rate acceleration in patients 1–3, but not in patient 4. Integrated SKNA (iSKNA) shows the total SKNA over 100 ms windows after applying 500 Hz high pass filter. HR= heart rate, bmp=beats per minute. (From Doytchinova et al, Heart Rhythm 2017)(47)

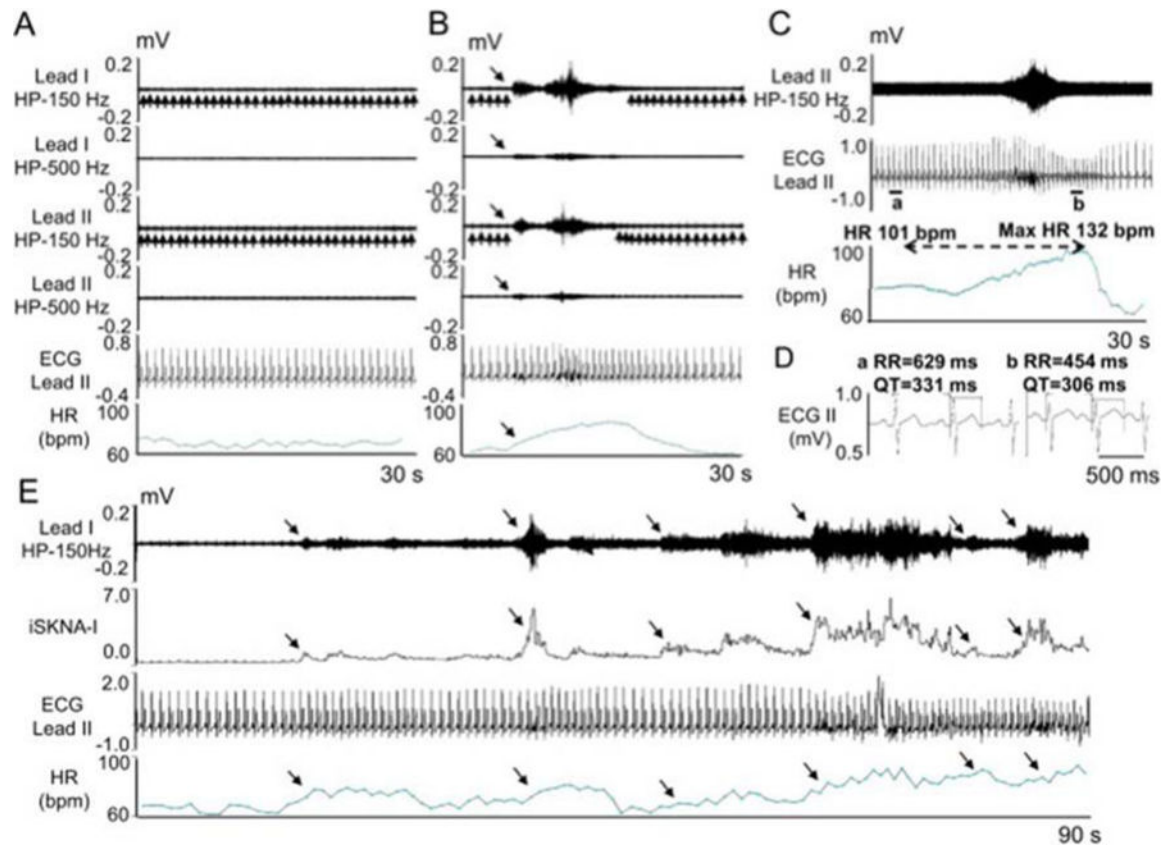


Figure 6.

SKNA recording in patients without known heart diseases. The electrodes were placed on the chest to form Lead I and Lead II. A - Baseline recording in leads I and II filtered at either 150 Hz or 500 Hz high pass to display SKNA and low pass filtered at 10 Hz to display the ECG. B - Episode of SKNA associated with heart rate (HR) acceleration (downward arrows). The 150 Hz high pass filter resulted in better signal to noise ratio and higher amplitude of SKNA, but some ECG signals remained (upward arrows). High pass filter at 500 Hz largely eliminated the ECG signals, but also reduced nerve amplitude and the signal to noise ratio. The baseline artifact on the surface ECG occurred after the onset of SKNA, suggesting motion artifacts induced by muscle movement. C - SKNA (500 Hz high pass, Lead II) and ECG tracings (125 Hz low pass) from a different patient. There was abrupt increase of HR from 101 beats per minute (bpm) to a maximum (1 max) of 132 bpm after SKNA activation, along with QT interval shortening. D - Enlarged ECG from line segments a and b in panel C. Both the RR and the QT interval shortened after SKNA. E - 90 s recording at baseline, illustrating spontaneous SKNA episodes and their relationship with HR. HP=high pass, LP=low pass, bpm=beats per minute. (From Doytchinova et al, Heart Rhythm 2017)(47)

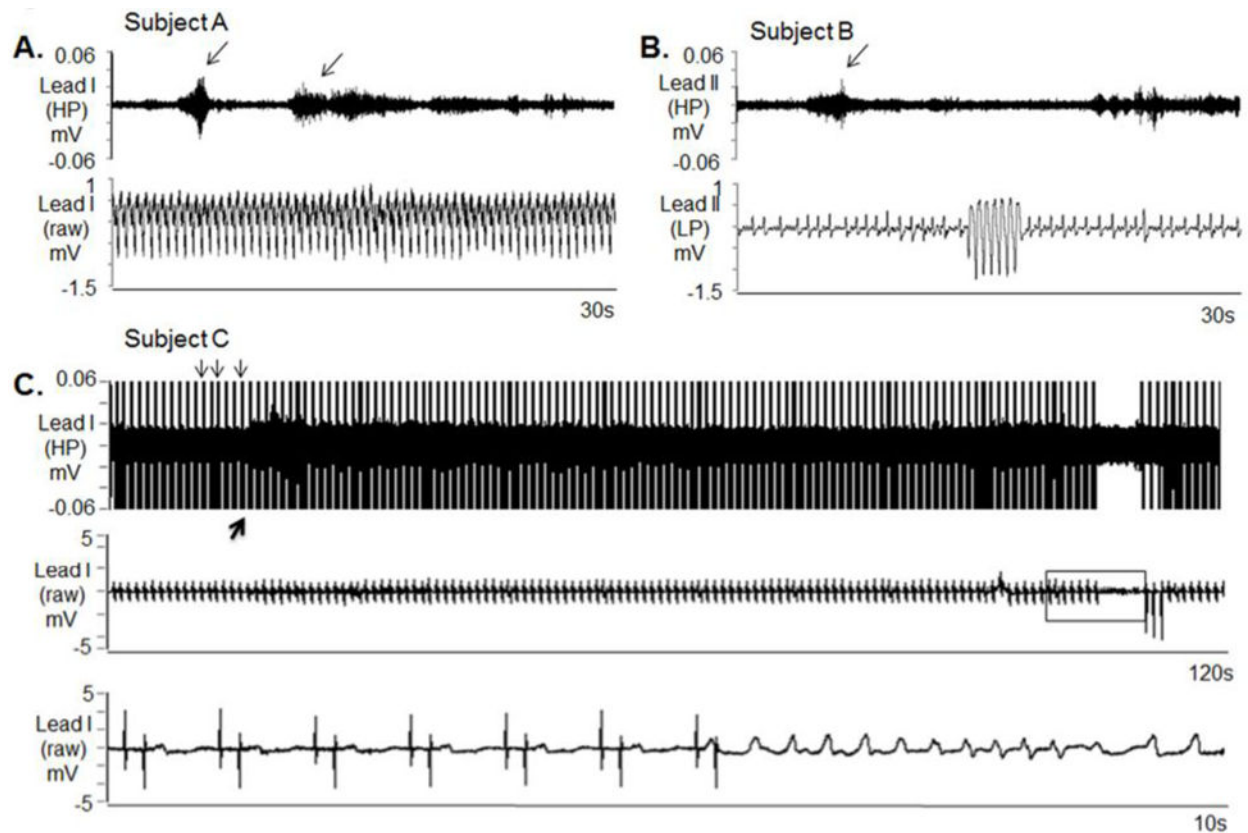


Figure 7.

SKNA during sustained VT and before nonsustained VT. The neuECG electrodes were placed on the chest to form Lead I and Lead II. A: Nerve discharges (arrows) are noted throughout monomorphic ventricular tachycardia (VT). Signals simultaneously obtained from ECG lead I with the top panel representing the signal after 500 Hz high pass (HP) filter and the bottom panel displaying the raw signal. B: Similar discharges are observed in another patient preceding non-sustained VT. Signal simultaneously obtained from ECG lead II, the top panel is filtered at 500 Hz high pass and the bottom ECG is filtered at 10 Hz low pass. C: Pacing artifacts (downward arrows) are observed despite 500 Hz high pass filtering. Increased high frequency SKNA is still evident (upward arrow) beginning 90 s prior to VT. The bottom panel shows the boxed segment from the middle panel and the onset of VT. VT=ventricular tachycardia, ECG=electrocardiogram, HP=500 Hz high pass filter, LP=10 Hz low pass filter, SKNA=skin sympathetic nerve activity. (From Doytchinova et al, Heart Rhythm 2017)(47)

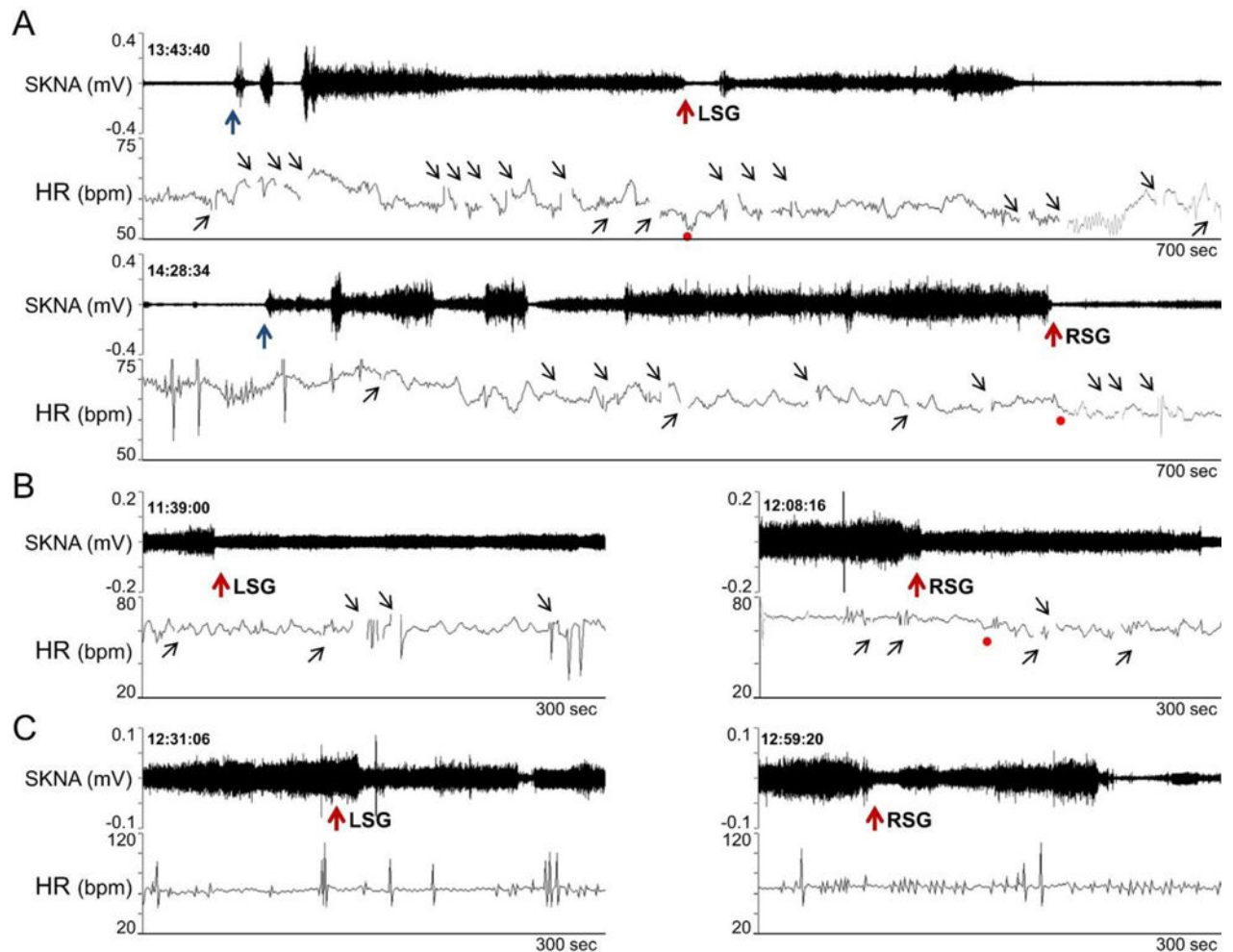


Figure 8. Effects of lidocaine (10 ml, 2 %) stellate ganglion block on SKNA continuously recorded from the right arm. A shows patient 1. Needle insertion (black arrows) was followed by activation of SKNA. Lidocaine injection (red arrows) into the LSG transiently reduced SKNA. However, RSG injection was followed by a significant reduction of SKNA. Panels B and C show responses to lidocaine injection in the remaining 2 patients. The gaps in tachogram (small black upward arrows) occurred because artifacts prevented automated selections of the R waves. (From Doytchinova et al, Heart Rhythm 2017)(47)